

This article was downloaded by:

On: 22 January 2011

Access details: *Access Details: Free Access*

Publisher *Taylor & Francis*

Informa Ltd Registered in England and Wales Registered Number: 1072954 Registered office: Mortimer House, 37-41 Mortimer Street, London W1T 3JH, UK



The Journal of Adhesion

Publication details, including instructions for authors and subscription information:

<http://www.informaworld.com/smpp/title~content=t713453635>

The Impact Resistance of Structural Adhesive Joints

A. J. Kinloch^a; G. A. Kodokian^a

^a Department of Mechanical Engineering, Imperial College, London, England

To cite this Article Kinloch, A. J. and Kodokian, G. A.(1987) 'The Impact Resistance of Structural Adhesive Joints', The Journal of Adhesion, 24: 2, 109 – 126

To link to this Article: DOI: 10.1080/00218468708075421

URL: <http://dx.doi.org/10.1080/00218468708075421>

PLEASE SCROLL DOWN FOR ARTICLE

Full terms and conditions of use: <http://www.informaworld.com/terms-and-conditions-of-access.pdf>

This article may be used for research, teaching and private study purposes. Any substantial or systematic reproduction, re-distribution, re-selling, loan or sub-licensing, systematic supply or distribution in any form to anyone is expressly forbidden.

The publisher does not give any warranty express or implied or make any representation that the contents will be complete or accurate or up to date. The accuracy of any instructions, formulae and drug doses should be independently verified with primary sources. The publisher shall not be liable for any loss, actions, claims, proceedings, demand or costs or damages whatsoever or howsoever caused arising directly or indirectly in connection with or arising out of the use of this material.

The Impact Resistance of Structural Adhesive Joints

A. J. KINLOCH and G. A. KODOKIAN

Department of Mechanical Engineering, Imperial College, London, SW7 2BX, England.

(Received December 10, 1986; in final form February 16, 1987)

The mechanical behaviour of structural adhesives and adhesive joints under impact loading is of growing interest as adhesives are used increasingly in the construction of vehicles ranging from the family motor car to large trucks and buses. The present paper describes some initial work on the development of an instrumented impact test to study the impact behaviour of epoxy adhesives and the use of a linear-elastic fracture-mechanics approach to characterising the fracture properties.

KEY WORDS Adhesive; impact; fracture; toughness; fracture energy; epoxy.

INTRODUCTION

When cured, epoxy resins are crosslinked polymers which are widely used as the basis for structural adhesives, especially when formulated to give a multiphase microstructure of rubbery particles in a matrix of thermoset epoxy since this may greatly increase the toughness of the adhesive.^{1,2} Such rubber-toughened adhesives are increasingly being used in general engineering applications, particularly in the manufacture of vehicles, and therefore their fracture behaviour under impact loading is of considerable interest.

The present paper describes the development of an instrumented impact test to assess the impact properties of adhesives and adhesive joints and the use of a linear-elastic fracture-mechanics approach to determine the fracture energy, G_{IC} . The merit of this

approach is that the value of G_{Ic} should be a 'material' characterising parameter, independent of the geometry of the specimen and hence can be extremely useful in the development and selection of adhesives and in engineering design.

EXPERIMENTAL

The materials

The structural adhesives examined were model materials based upon a simple, unmodified and a rubber-toughened epoxy resin. The epoxy resin was derived from the reaction of bisphenol A and epichlorohydrin and was largely composed of the diglycidyl ether of bisphenol A (DGEBA). The curing agent was piperidine. The rubber used to prepare the multiphase, rubber-modified epoxy adhesive was a carboxyl-terminated, random copolymer of butadiene and acrylonitrile (CTBN rubber; carboxyl content 2.37 wt/wt%; molecular weight 3500 gmol^{-1}). The formulations of the epoxy adhesives are shown in Table I.

Preparation of bulk specimens

Bulk specimens of the adhesives were tested in the form of single-edged notched three-point bend (SENB) specimens, shown schematically in Figure 1. The SENB specimens were manufactured by first casting sheets of the epoxy polymers which were 10 mm in thickness. The casting mixture was prepared by adding the CTBN rubber to the epoxy resin and hand-mixing for approximately 5 to 10 min. This mixture was then heated to $65 \pm 5^\circ\text{C}$ in a water bath

TABLE I
Formulations of epoxy adhesives

	Unmodified epoxy (phr*)	Rubber-modified epoxy (phr)
DGEBA epoxy resin	100	100
Piperidine	5	5
CTBN rubber	—	15

* phr = parts per hundred of resin

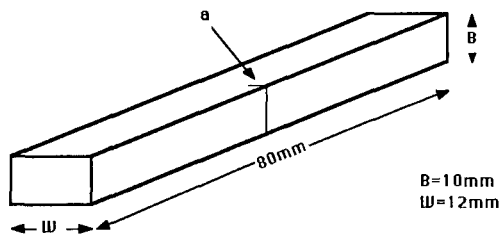


FIGURE 1 Sketch of single-edged notched three-point bend (SENB) bulk specimen.

and mixed for 5 min using an electric stirrer and then degassed in a vacuum oven at 60°C until frothing stopped. When the mixture had cooled to below 30°C the piperidine was mixed in gently to minimise air entrapment. The rubber-epoxy mixture was then poured into a preheated mould, cured at 120°C for 16 h (no exotherm being recorded) and allowed to cool slowly. The unmodified epoxy was prepared in the same manner without the addition of rubber. The formulation and cure schedule described above results^{3,4} in reproducible materials with the rubber-modified epoxy material having a two-phase microstructure with a volume fraction of rubbery particles of 0.18 with an average particle size of $1.6\ \mu\text{m}$. The glass-transition temperature of the epoxy is $100 \pm 2^{\circ}\text{C}$.

The SENB specimens were prepared by machining the sheets of epoxy polymer into bars of the dimensions shown in Figure 1. Cracks were then inserted into the bars by either machining a notch using a narrow milling cutter (termed a 'flycutter') of known radius or by machining a notch of radius approximately $12\ \mu\text{m}$ and then gently tapping a fresh razor blade into the notch so as to propagate a sharp, natural crack ahead of the razor blade. Cracks of various lengths, a , were inserted using these techniques.

Most of the test specimens had a crack initiation gauge applied to one surface so that the onset of crack growth, and the associated force at this point, could be accurately determined. The design of the gauge followed closely that described by Beguelin, *et al.*⁵ One face of the specimen, of length W and perpendicular to the face across which the crack was inserted, was drilled to accommodate two small pins, which were pushed into place one on each side of the crack and about 10 mm from the crack. Then a graphite polymeric-based film was sprayed completely across the width of the

specimen to give a thin, uniform graphite film to a distance of about 1.5 to 2 mm on either side of the crack. The gauge was finished by painting a thin line of conductive silver paint over the top of the far edge by the graphite layer, *i.e.* completely across the width of the specimen, and then on each side of the crack a silver path was painted to the pin which had been mounted on that half of the specimen.

Adhesive joint specimens

Adhesive joint specimens were prepared in the form of SENB specimens, as shown schematically in Figure 2, and these consisted of bonded bars of aluminium-alloy which were $39.25 \times 12 \times 8$ mm. Prior to being bonded the end faces of the aluminium-alloy bars were surface treated by etching in chromic-acid (prepared according to the optimised Forest Products Laboratory (FPL) specification⁶) at 68°C for 20 mins. They were then rinsed thoroughly in tap water and dried. The aluminium-alloy bars were then placed in a rubber mould with a gap of 1.5 mm between them and heated to 120°C . Rubber-modified epoxy mixture was then prepared as described above and poured carefully into the gap to form a joint. The adhesive was cured by heating at 120°C for 16 h. The joint was then removed from the mould and a crack machined into the centre of the adhesive using a slender flycutter with a radius of $12\ \mu\text{m}$. It should be noted that the insertion of sharper cracks using a razor blade was attempted but was not successful, although this technique did work successfully in the case of the bulk specimens. This difficulty possibly arose from the higher stiffness of the joint

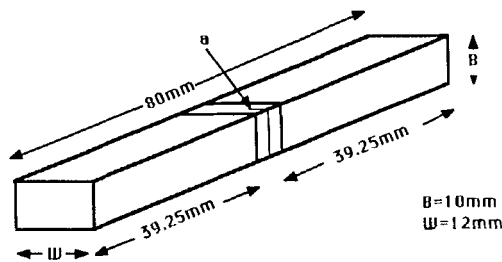


FIGURE 2 Sketch of single-edged notched three-point bend (SENB) adhesive joint specimen.

specimens, which leads to a greater tapping force being required to insert a natural crack when using the razor blade technique. This, in turn, appeared to make the control necessary to propagate only a short crack, rather than have the crack propagate completely through the specimen, impossible to achieve.

As for the bulk SENB specimens, a crack initiation gauge was applied across the crack so that the associated force at the onset of crack growth could be accurately determined.

The instrumented impact test equipment

The impact tests were conducted using a commercial instrumented machine (Ceast, Turin, Italy). It essentially consisted of a pendulum-striker which was allowed to impact against the specimen. The velocity with which the striker hit the specimen could be varied by changing the angle from which the striker was released and the strain-gauge transducer was mounted in the striker. This force transducer was connected to a transient recorder and therefore, through a prior static calibration, the impact force *versus* time signal could be obtained. The memory module received the signal converted by the analogue/digital converter into digital form, and stored these data. The time-base generator was based upon intervals of 2-4-8-16-32-64-124-256 ms and each of these was divided into 2016 points so that the time interval between two bits (information) was included between 1 and 126 μ s. By adjusting the trigger system according to the duration of the phenomenon, the memory module could store the complete force *versus* time history of the impact experiment. These data could be accessed by the dedicated microcomputer. It should be noted that throughout these studies no filtering of the force *versus* time signal was performed since, although the equipment had this capability, it was considered that vital information might be lost by such an operation.

As mentioned above, it was also considered to be essential to be able to discern the point on the measured force *versus* time curve that the inserted starter crack began to propagate. To determine this point the crack initiation gauge was connected to a balancing bridge which gave a constant voltage. The signals from both the balancing bridge and the transient recorder which was used to store the force *versus* time data were connected to a second transient

recorder to produce, on the same time-scale axis, both changes in the force (from the semi-conductor strain gauge) and resistance (from the crack initiation gauge) as a function of time. These data could be accessed *via* an *X-Y* plotter.

The fracture tests

The bulk or the joint SENB specimen was placed on the shoulders of the vice of the instrumented impact machine to give a span of 48 mm and was struck by the pendulum-striker on the reverse face to that containing the inserted crack. Low impact velocities, typically about 0.5 m/s, were used so as to keep the well-reported⁷⁻⁹ dynamic effects to a minimum. In the case of the bulk adhesive specimens the effect of employing relatively high impact velocities has been the subject of another publication.⁹ It is sufficient to note that at higher velocities the dynamic effects caused by the specimen accelerating and decelerating relative to the striker led to many large oscillations in the measured force *versus* displacement trace and to the measured force on the striker being very different in value from the force acting in the specimen. Since the accurate determination of the fracture energy requires a knowledge of the force acting in the specimen, this obviously leads to misleading estimates of the value of G_{Ic} . However, an impact velocity of about 0.5 m/s generally results in a sufficiently long time-scale for the impact event such that these dynamic effects are minimal. Further, it should be noted that the test specimens examined in the present work are relatively very stiff, unlike most real practical joint designs. Thus, the relatively low impact velocities used in the present study do in fact result in times-to-failure and strain rates of direct relevance to the impact behaviour of bonded engineering structures.

The strain-gauge transducer was mounted in the top of the pendulum-striker and a record of the force *versus* time and resistance of the crack initiation gauge *versus* time were recorded as described above. Apart from enabling direct graphical representation of the force *versus* time data received and hence determination of the force, F_c , at the onset of crack growth, the computer was programmed to deduce various other parameters of interest. The equations used were simply based upon Newtonian

mechanics and required a knowledge of the initial impact velocity and the mass of the pendulum-striker. Assuming that no dynamic effects, such as those described earlier, are experienced (so that the energy lost by the striker may be equated to that gained by the specimen), then the equations used in the program yielded (i) the energy, U , absorbed by the specimen as a function of time, (ii) the displacement, u , of the specimen as a function of time and (iii) the force, F , versus displacement, u relation.

The above experiments were conducted over a range of test temperatures from 60°C to -40°C.

Calculation of the fracture energy

The fracture energy, G_{Ic} , is given from a linear-elastic fracture-mechanics (LEFM) analysis by¹⁰:

$$G_{Ic} = \frac{F_c^2}{2B} \frac{\partial C}{\partial a} \quad (1)$$

where F_c is the force at the onset of crack growth, B is the thickness of the specimen and C is the compliance of the test specimen which is given by the displacement/load (*i.e.*, u/F). If a dimensionless geometric factor, Φ , is introduced such that¹¹:

$$\Phi = \frac{C}{\partial C / \partial (a/W)} \quad (2)$$

where W is the width of the specimen, it may be readily shown that¹¹:

$$G_{Ic} = \frac{U_c}{BW\Phi} \quad (3)$$

where U_c is the stored elastic strain-energy at the onset of crack growth. The value of Φ may be evaluated either from measuring the compliance as a function of crack length or, more readily, from published tables¹¹ of the value of Φ as a function of a/W and L/W , where L is the length or span of the test specimen between the supported points.

RESULTS AND DISCUSSIONS

Applicability of LEFM

Typical force *versus* time (from the force transducer) and resistance *versus* time (from the crack initiation gauge) traces from impact tests conducted on bulk and joint SENB specimens are shown in Figures 3a and b respectively. In both cases the force *versus* time

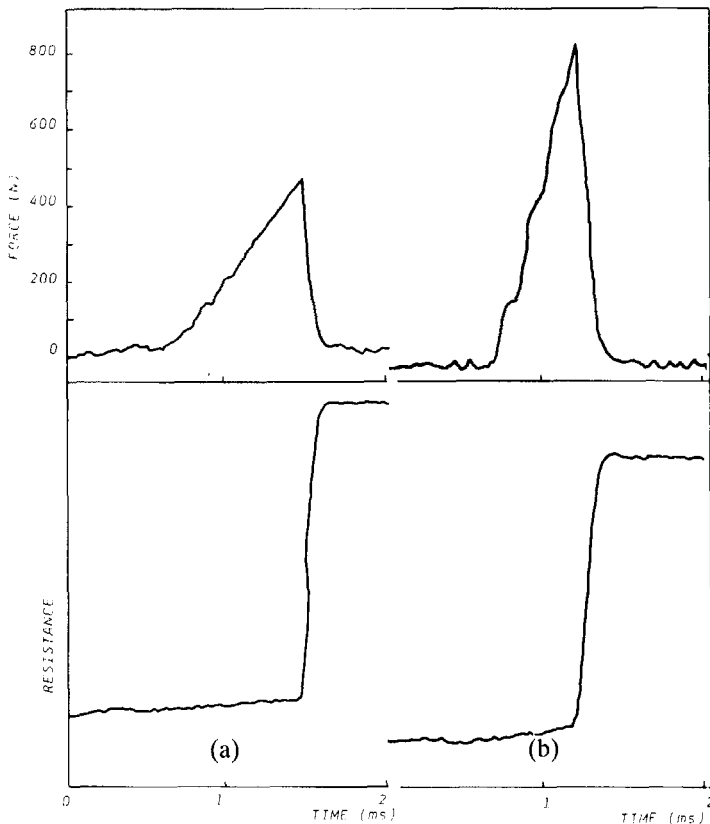


FIGURE 3 Force *versus* time (from the striker transducer) and resistance *versus* time (from the crack initiation gauge) traces. (Striker velocity 0.5 m/s; crack tip radius 12 μm ; test temperature 20°C.) (a) Bulk rubber-modified SENB specimen. (b) Adhesive joint rubber-modified SENB specimen.

trace does exhibit a few oscillations arising from the dynamic effects described above but they have disappeared by the time that the resistance *versus* time trace reveals that the crack starts to propagate. Also, it is important to note that the crack initiation gauge clearly demonstrates that crack growth is not associated with these oscillations, as might have been the interpretation without the benefit of the gauge. Indeed, the gauge indicated that the onset of crack growth invariably occurs at the maximum recorded force, except at above ambient test temperatures when the onset of crack growth is just prior to the maximum force recorded.

To examine the applicability of LEFM theory to the impact tests the measured energy, U_c , at the onset of crack growth was plotted against the corresponding value of the term $BW\Phi$, a wide range of Φ values being generated by inserting cracks of different length into the SENB specimens. Obviously, from Eq. (3) such plots should be linear, passing through the origin, to give a value of the fracture energy, G_{Ic} , which is independent of test geometry. Some typical plots are shown in Figure 4 and in all cases the experimental data provides a good fit to the LEFM theory as stated in Eq. (3). The exact test conditions are indicated in Figure 4 and the value of the time-to-failure, t_f , is defined as the time taken for the value of the measured force to increase from $F=0$, at the start of the force *versus* time curve, to $F=F_c$.

A second approach to determining the value of G_{Ic} from the measured data is to use Eq. (1). This requires the compliance, C , of the specimen to be assessed and for the instrumented impact tests this may be readily undertaken since the force versus displacement relation can easily be obtained, as described above. Figure 5 shows a plot of $F_c^2/2B$ *versus* $(\partial C/\partial a)^{-1}$ and again a good linear relation, passing through the origin, is observed. Good agreement between the values of G_{Ic} from Eqs (1) and (3) are recorded and, for the example given in Figure 5, the values obtained from these two equations are 1.43 and 1.31 kJ/m² respectively.

Finally, it should be noted that the value of the stress-intensity factor, K_{Ic} at crack initiation may, in theory, be deduced from the measured force, F_c , using equations of the form:

$$K_{Ic} = \sigma_c Y \sqrt{a} \quad (4)$$

where σ_c is the applied stress at the onset of crack growth and Y is

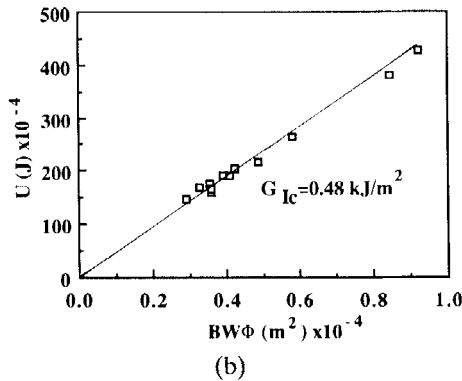
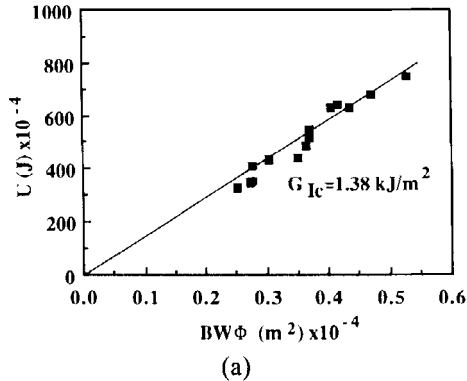


FIGURE 4 Plots of the energy, U_c , absorbed by the specimen up to the onset of crack growth versus $BW\Phi$. (a) Bulk rubber-modified epoxy SENB specimen; striker velocity 0.5 m/s; $t_f = 930 \mu\text{s}$; crack tip radius naturally sharp; 20°C. (b) Bulk unmodified epoxy SENB specimen; striker velocity 0.33 m/s; $t_f = 800 \mu\text{s}$; crack tip radius naturally sharp; 20°C. (c) Bulk rubber-modified epoxy SENB specimen; striker velocity 0.5 m/s; $t_f = 755 \mu\text{s}$; crack tip radius naturally sharp; -20°C. (d) Adhesive joint rubber-modified epoxy SENB specimen; striker velocity 0.5 m/s; $t_f = 380 \mu\text{s}$; crack tip radius 12 μm ; -20°C.

the geometry factor. The value of K_{Ic} may be related to the value of G_{Ic} by an equation of the form:

$$K_{Ic}^2 = EG_{Ic} \quad (5)$$

where E is a modulus function. In the case of the bulk specimens the above equations are straightforward and may be readily employed, as discussed in other publications^{9,12}. However, for the

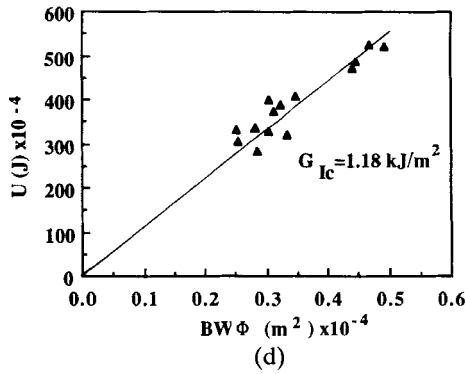
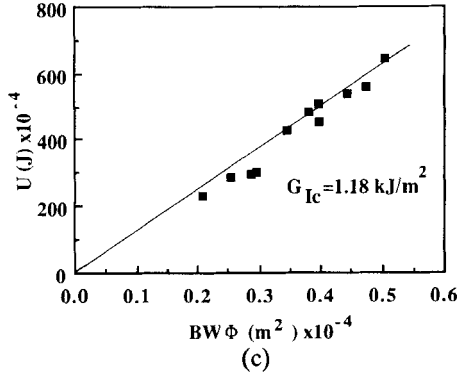


FIGURE 4 (Continued)

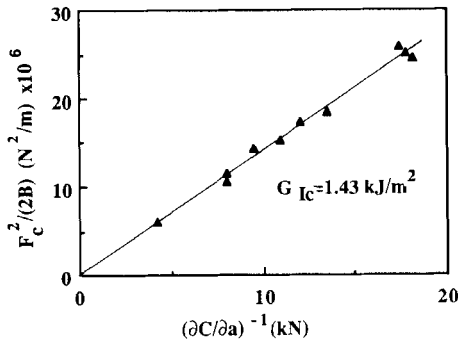


FIGURE 5 $F_c^2/2B$ versus $(\partial C/\partial a)^{-1}$ for an adhesive joint bonded with the rubber-modified epoxy. (Striker velocity 0.5 m/s; crack tip radius $12 \mu\text{m}$; 20°C).

adhesive joints the geometric term is an unknown function of the thickness of the adhesive layer, amongst other parameters, and can only be readily ascertained by a complex numerical analysis. It cannot be assumed to be of the same value as that for the bulk homogeneous material, and in most instances it is, indeed, different. Further, the value of the modulus function is dependent upon where the crack propagates, *i.e.* whether interfacially or in the adhesive layer. These problems have been reviewed in depth elsewhere¹ and in the present studies the former problem is particularly difficult to resolve. Therefore, the authors have adopted the approach that the fracture energy, G_{Ic} , is a more suitable fracture mechanics parameter than the stress-intensity factor, K_{Ic} , since it may be defined unambiguously and calculated directly from the experimental data.

The present data have established the soundness of the experimental techniques and the validity of a LEFM approach. In the following Sections the effects of various test parameters and a comparison of the bulk *versus* joint impact behaviour are discussed.

Effect of crack tip radius on the value of G_{Ic}

In the case of the bulk rubber-modified epoxy SENB specimens the value of the fracture energy, G_{Ic} , was determined as a function of the initial tip radius of the inserted crack. An impact velocity of 0.5 m/s was employed and the results are illustrated in Figure 6.

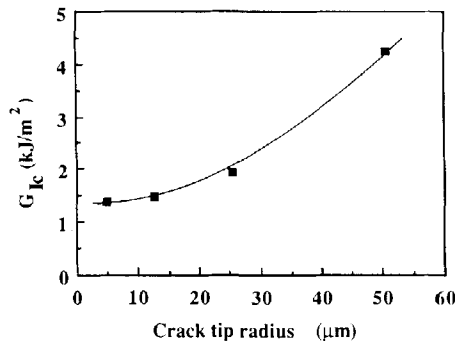


FIGURE 6 Effect of tip radius of inserted starter crack on the measured fracture energy. (Bulk rubber-modified SENB specimens; striker velocity 0.5 m/s; 20°C).

The value of G_{Ic} shown for a tip radius of about $5\ \mu\text{m}$ is that obtained from the natural crack, whilst the other values have been obtained using flycutters of various tip radii. As would be expected, the value of G_{Ic} increases as the crack tip radius increases, *i.e.* as a blunter initial starter crack is employed. However, when the cracks are relatively sharp, there is not a large difference between the G_{Ic} value obtained from the naturally sharp crack induced *via* the razor blade technique and that obtained *via* using a sharp flycutter having a tip radius of approximately $12\ \mu\text{m}$. This observation has important consequences since values of the fracture energy should be quoted for naturally sharp cracks. This will give the minimum, lower-bound, values of G_{Ic} and it is these values which should be used for adhesive development and selection purposes and design studies.

It was not found possible to insert naturally sharp cracks into the adhesive layer in the joints but the above results demonstrate that the value of G_{Ic} for the adhesive joints prepared using the rubber-modified adhesive will not be significantly overestimated if cracks are inserted using the sharpest flycutter, having a tip radius of about $12\ \mu\text{m}$. It should be noted, however, that this observation will only be valid for the tough adhesives which are relatively insensitive to the sharpness of the initial crack, providing the crack tip radius is relatively small. In the case of the more brittle unmodified epoxy, the use of even the sharpest flycutter resulted in values of G_{Ic} considerably greater than that obtained using a naturally sharp crack.

Therefore, in the work described below the bulk specimens of unmodified and rubber-modified epoxy contained naturally sharp cracks and only joints prepared using the rubber-modified epoxy were tested and these contained cracks which had been inserted by employing the sharpest flycutter.

Effect of test temperature on the value of G_{Ic}

Values of G_{Ic} are shown as a function of test temperature in Figure 7 for bulk and adhesive joints prepared from the rubber-modified epoxy and bulk unmodified epoxy specimens. A striker velocity of $0.5\ \text{m/s}$ was employed in all these studies. Several interesting features emerge from the data shown in Figure 7.

Firstly, the values of G_{Ic} for bulk and joint specimens are in very

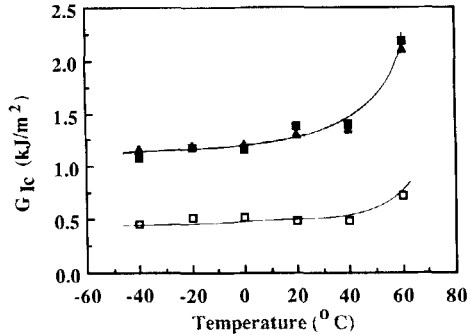


FIGURE 7 The fracture energy, G_{Ic} , as a function of test temperature. (Striker velocity 0.5 m/s). ■ Bulk rubber-modified epoxy. ▲ Adhesive joints (rubber-modified epoxy). □ Bulk unmodified epoxy.

close agreement for the rubber-modified adhesive. This result is not unexpected since the locus of joint failure was by crack growth through the adhesive layer, away from the adhesive/aluminium oxide interface and the adhesive layer was relatively thick compared to the expected crack-tip plastic-zone size.^{1,13,14} Some workers¹ have argued that a relatively thin film of adhesive material in a joint may not behave the same as a thick bulk specimen but, as noted above, the crack growth was not close to either interface and therefore a good correlation between the fracture behaviour of the adhesive and bulk specimens is not surprising.

Secondly, at all the test temperatures, the rubber-modified epoxy is significantly tougher than the unmodified epoxy. This arises from the main energy-dissipating micromechanism at the crack tip involving shear deformations in the epoxy.¹⁻³ The extent of such deformations are very limited in the unmodified material but occur over a large volume in the rubber-modified material, since many such deformations are initiated by the rubbery particles which are present in this adhesive. The increased plastic and viscoelastic energy which is dissipated at the crack tip by this multiple-deformation micromechanism is reflected by an increase in the value of G_{Ic} . Even at the lowest test temperature of -40°C the rubber-modified adhesive is approximately two to three times tougher than the unmodified material.

Thirdly, the value of G_{Ic} for the rubber-modified adhesive is

significantly dependent upon the test temperature, with the value of G_{Ic} increasing as the temperature is increased. As the test temperature is increased the stress at which shear yielding occurs decreases and shear deformations can, therefore, occur more readily. Again, the increased plastic and viscoelastic energy which is dissipated at the crack tip is reflected by an increase in the value of G_{Ic} . A similar, but less marked trend, is observed for the unmodified epoxy material. The reason that it is more marked for the rubber-modified material probably arises from the rubbery particles in the rubber-modified material cavitating at the higher test temperatures, as may be seen both by the presence of stress-whitening and by observation of the fracture surfaces in the scanning electron microscope. This cavitation process relieves the degree of triaxiality in the tensile stress field at the crack tip which, in turn, enables further shear deformations to occur in the epoxy matrix. This further enhances the toughness of the rubber-modified epoxy compared to the unmodified epoxy.

Comparison between impact and slow strain-rate values of G_c

Values of the fracture energy, G_{Ic} , for the rubber-modified epoxy from the impact test described above and from slow-rate tests, conducted using an Instron tensile testing machine, are compared in Table II.

TABLE II
Comparison of slow-rate and impact tests for the rubber-modified adhesive

Test temp. (°C)	Fracture energy, G_{Ic} (kJ/m ²)			
	Slow-rate		Impact	
	Bulk	Joint	Bulk	Joint
-40	0.75	—	1.08	1.17
-20	1.10	—	1.18	1.18
0	1.36	—	1.17	1.19
20	1.88	1.89	1.38	1.31
40	3.76	—	1.40	1.39
60	6.29	—	2.18	2.10

Notes: (i) Slow-rate tests conducted at a displacement rate of 1.67×10^{-5} m/s, giving typical values of t_f of between 30 to 300 s. (ii) Impact tests conducted at a striker velocity of 0.5 m/s, giving typical values of t_f of between 400 to 1000 μ s. (iii) Joints failed by cohesive fracture in the adhesive layer.

Several interesting points are evident from the data shown in Table II. Firstly, there is very good agreement between the values of G_{Ic} for the bulk and adhesive joint specimens, as commented previously.

Secondly, at the lowest test temperatures there is only a small difference between the values from the slow-rate and impact tests. This is in accord with previous results³ where the effect on the value of G_{Ic} over a range of relatively slow rates of test was examined and it was found that at low temperatures the effect of test rate was not very marked. However, it is interesting to note that at these low temperatures the values of G_{Ic} from the impact tests may even be somewhat greater than those from the slow-rate tests. This could result from the relatively very short time-to-failure, t_f , values incurred in the impact tests at these low temperatures; for example the value of t_f is typically about 700 μ s for the bulk SENB specimens at -40°C but about 1750 μ s at 60°C . Such very short failure times at the low test temperatures might result in some dynamic effects being still felt when crack initiation occurs. Alternatively, some local adiabatic heating¹⁵ might occur at the crack tip which would cause a local decrease in the stress for shear yielding and a local toughening effect. Whatever the cause, the value of G_{Ic} from the impact test does certainly appear to be somewhat greater than the value from the slow-rate test at a test temperature of -40°C .

Thirdly, at temperatures above about 0°C the value of G_{Ic} from the impact test is now undoubtedly lower than the corresponding value from the slow-rate test, and the difference between the values increases as the test temperature is increased. At these higher test temperatures the rubber-modified epoxy when tested at slow rates shows clear evidence of extensive cavitation occurring in the rubbery particles. However, in the impact tests the cavitation of the rubbery particles is observed to be far more limited. The much lower extent of cavitation may be associated with the time of the impact event being too short to enable this micromechanism to proceed readily, *i.e.* a kinetic controlling factor. For the reasons discussed above, the lower extent of cavitation observed in the impact tests at higher temperatures will lead to less energy dissipation around the crack tip and hence a lower value of G_{Ic} . It is interesting to observe how marked the effect of rate of test on the value of G_{Ic} is at the highest test temperature of 60°C . At this

temperature the value of G_{Ic} from the slow-rate test is greater by a factor of about three. Considering the general applicability of this observation to other rubber-toughened adhesives, it should be noted that previous work^{3,4,16,17} has revealed that when the difference between the test temperature and the glass-transition temperature of the epoxy is less than about 100°C then at slow rates of test the extent of the cavitation micromechanism and the toughness of the material begins to increase more rapidly as the test temperature is further progressively raised. Hence, as the glass-transition temperature of the epoxy is approached it would be expected that the difference between the values of G_{Ic} from slow-rate and impact tests will be greatest, as indeed observed in the present work.

CONCLUSIONS

The present studies have described the development of an instrumented impact test which may be used to study the crack growth behaviour in structural adhesives and adhesive joints. Further, it has been shown that, when dynamic effects are avoided, the data from such tests may be used together with a linear-elastic fracture-mechanics approach to yield valid values of the fracture energy, G_{Ic} .

Values of the fracture energy, G_{Ic} , under impact loading have been found to be the same for bulk specimens and adhesive joints prepared using a rubber-modified epoxy—the joints having been prepared with relatively thick adhesive layers and the locus of joint failure being *via* crack growth through the adhesive layer. The values of G_{Ic} for the rubber-toughened epoxy adhesive are always significantly greater than those for the unmodified epoxy, even at the lowest test temperature of -40°C.

Comparison of the impact values of G_{Ic} with those obtained from slow-rate tests, where the time-to-failure was typically about three orders of magnitude longer, has revealed that, except at the lowest test temperatures, the values of G_{Ic} are significantly lower when measured under impact conditions. The difference between the values of G_{Ic} from the impact and the slow-rate tests is greatest at the higher test temperatures, *i.e.* as the glass-transition temperature of the epoxy is approached.

Finally, although the impact velocities used in the present study have been deliberately kept low, to avoid gross dynamic effects, higher impact velocities may be used with the test equipment described in the present paper. However, under such conditions the dynamic effects need to be modelled and accounted for if valid, 'material' characteristic values of G_{1c} are to be deduced, as described elsewhere.⁹

Acknowledgement

The authors would like to thank the Science and Engineering Research Council, through the Polymer Engineering Directorate, for financial support.

References

1. A. J. Kinloch, *Adhesion and Adhesives: Science and Technology* (Chapman Hall, London, 1987).
2. A. J. Kinloch, *Structural Adhesives: Developments in Resins and Primers*, A. J. Kinloch, Ed. (Elsevier Applied Science, London, 1986), p. 127.
3. A. J. Kinloch, S. J. Shaw, D. A. Tod and D. L. Hunston, *Polymer* **24**, 1341 (1983).
4. A. J. Kinloch and D. L. Hunston, *J. Mater. Sci. Lettrs.* **6**, 131 (1987).
5. Ph. Beguelin, B. Stalder and H. H. Kausch, *Int. J. Fracture* **22**, R47 (1983).
6. J. C. McMillan, *Bonded Joints and Preparation for Bonding*, NATO, AGARD Lecture Series No. 102, (NATO, AGARD, France, 1979), p. 7.1.
7. J. F. Kalthoff, *Int. J. Fracture* **27**, 277 (1985).
8. J. G. Williams and G. C. Adams, *Int. J. Fracture*, to be published.
9. A. J. Kinloch, G. A. Kodokian and M. B. Jamarani, *J. Mater. Sci.*, to be published.
10. A. J. Kinloch and R. J. Young, *Fracture Behaviour of Polymers* (Applied Science, London, 1983), p. 74.
11. J. G. Williams, *Fracture Mechanics of Polymers* (Ellis Horwood, Chichester, 1984), p. 62.
12. A. J. Kinloch and G. A. Kodokian, *J. Mater. Sci. Lettrs.*, to be published.
13. A. J. Kinloch and S. J. Shaw, *J. Adhesion* **12**, 59 (1981).
14. W. D. Bascom and R. L. Cottingham, *J. Adhesion* **7**, 333 (1976).
15. J. G. Williams and J. M. Hodgkinson, *Proc. Roy. Soc., London*, **A375**, 231 (1981).
16. D. L. Hunston, A. J. Kinloch, S. J. Shaw and S. S. Wang, in *Adhesive Joints*, K. L. Mittal, Ed. (Plenum Press, New York, 1984), p. 789.
17. L. C. Chan, J. K. Gillham, A. J. Kinloch and S. J. Shaw, *Rubber-Modified Thermoset Resins*, C. K. Riew and J. K. Gillham, Eds. (American Chemical Soc., Washington, 1984), p. 261.